Rare Earth doped silicate glass-ceramics for LED application

I. Koseva[1], P. Tzvetkov[1*], P. Ivanov[2], A. Yordanova, V. Nikolov[1]

[1] *Institute of General and Inorganic Chemistry, Bulgarian Academy of Sciences, 1113 Sofia, Bulgaria*
[2] *Institute of Optical Materials and Technology, Bulgarian Academy of Sciences, 1113 Sofia, Bulgaria*

Rare earth doped glasses from the system Li_2O-Al_2O_3-SiO_2-$LiBO_2$ (19.6:19.6:39.1:21.7 mol%) are prepared with concentration of the dopants 0.5 at.% for Tb^{3+} and 0.1 at.% for Eu^{3+}. Glass-ceramics are obtained after thermal treatment of the parent glass at two different temperatures (580 and 630 °C) and for three different durations (2, 5 and 24 hours). The crystallizing phases, the crystallization degree and the particle size are determined. The main crystallizing phase after thermal treatment with different duration time is $LiAlSiO_4$ in two different structural modifications – β-Eucryptite and γ-Eucryptite. Powder XRD analyses show the presence of additional phases with quantity less than 5%. The crystallinity of all samples is about 90%. The particle size depends slightly on the Rare Earth ion and varies between 80 and 120 nm according to the thermal treatment regime. Emission and excitation spectra of the glass-ceramics show the characteristic peaks of Tb^{3+} and Eu^{3+}. The main emission peak of Tb^{3+} is $^5D_4 \rightarrow {}^7F_5$ transition at 545 nm, corresponding to green color. The main emission peak of Eu^{3+} is $^5D_0 \rightarrow {}^7F_2$ transition at 613 nm, corresponding to orange-red color. CIE coordinates of the samples show different emission colors, which depend on the active ion and the thermal treatment regime. The obtained results show that as-prepared terbium doped glass-ceramics could be used as a blue-green phosphor. Europium doped glass-ceramics could be used as an orange-red phosphor. Different emission colors could be obtained by using different thermal treatment regimes.

Keywords: silicate phosphor, nano glass-ceramic, Rare-Earth ions, X-ray, photoluminescence.

INTRODUCTION

Light emitting diodes as an energy and environment saving devices are of special interest and become more and more popular in the modern life [1, 2]. Different colors are obtained by doping with different ions [3–10] or mixing of multicolor phosphors [11–15]. For example, white light emitting diodes can be realized by combining the emission of blue and yellow phosphors or by mixing the emission of blue, green and red phosphors [1, 16]. The luminescence of the rare earth ions strongly depends on the concentration of the activator, composition and crystal structure of the host and on preparative method [16]. Silicates are one of the most suitable materials because of their high chemical and mechanical stability and various crystal structures [2]. Silicate, silicate glasses and glass-ceramics doped by rare earth ions are among the most popular materials for optical fibers, LEDs, wave guides for optoelectronic communication and color display devices. Rare earth doped glass ceramics are a good

alternative to conventional phosphors and glasses because of the low cost preparation process, simple manufacturing procedure and free from the halo effect. Mechanical, thermal, electrical and optical properties of the material could be improved by controlled heat treatment of the parent glass [17–19]. Therefore, many investigations are realized and published in recent years on doped silicate glass-ceramics [19–24].

Tb^{3+} doped phosphor materials possess a strong excitation band in the near UV region (around 379 nm) and show green emission due to $^5D_4 \rightarrow {}^7F_5$ (545 nm) transition. In lower concentrations of the Tb^{3+} ion (in order of 1%) it also emitted from the higher levels in the blue region of the spectra. When the concentration of Tb^{3+} ion is lower, Tb–Tb distances are large and emission from the $^5D_3$ and $^5D_4$ excited states is observed. At higher Tb concentrations, cross-relaxation quenches the emission from the $^5D_3$ levels. Eu^{3+} doped phosphor materials possess an excitation band in the near UV light (around 400 nm) and show orange-red emission corresponding to $^5D_0 \rightarrow {}^7F_1$ (592 nm) or $^5D_0 \rightarrow {}^7F_2$ (612 nm) transitions. Their photoluminescence emission strongly depends on the symmetry of the crystal structure of the host. If the Eu^{3+} ions occupy the sites with in-

---

* To whom all correspondence should be sent:
E-mail: tzvetkov@svr.igic.bas.bg

version symmetry, the emission is from the $^5D_0 \rightarrow {}^7F_1$ magnetic-dipole transition in the range 590–600 nm. This emission is not affected much by the site symmetry. The emission at approximately 612 nm is due to the $^5D_0 \rightarrow {}^7F_2$ electric dipole transition and will dominate if the Eu^{3+} ion occupies the site without inversion symmetry [5, 9, 16, 25].

Our previous investigations on the system Li_2O-Al_2O_3-SiO_2-$LiBO_2$ revealed us an opportunity to obtain glass-ceramics containing $LiAlSiO_4$ as a main crystallizing phase [26].

$LiAlSiO_4$ is a technologically relevant ceramic, owing to its near to zero thermal expansion coefficient, great thermal and chemical shock resistance, exceptional thermal stability. Up to now, this material is used not only in the field of domestic cookware, but also for various specific applications like heat exchangers, ring laser gyroscopes, precision optical devices and radiation dosimetry purposes [27].

The $LiAlSiO_4$ structure has been studied by Winkler and has been confirmed by Roy et al. [28, 29]. High eucryptite, $LiAlSiO_4$, is isomorphous with high quartz, where half of the Si atoms are replaced by Al forming the three-dimensional network of corner-sharing AlO_4 and SiO_4 tetrahedra. The Li^+ ions are placed in void channels within the spirals of $(Si,Al)O_4$ tetrahedra. According to Schulz, the unit cell is with hexagonal symmetry ($P6_222$) [30, 31]. The high eucryptite form is stable on cooling even with prolonged heating at low temperatures [32]. Roy et al. also established the reconstructive inversion of the high eucryptite to the rhombohedral phenacite type of low eucryptite (α-eucryptite) at 972° ± 10 °C. At about 650 °C γ-eucryptite is formed, and its structure is monoclinic with space group *Pa*. At 900–1000 °C γ-eucryptite transforms into the final high-temperature polymorph β-eucryptite [33, 34].

Only one article is published on doping of $LiAlSiO_4$ by rare earth ion (Sm^{3+}) [35]. The compound is synthesized by conventional solid state technique.

In this paper, we report obtaining of Tb^{3+} doped and Eu^{3+} doped $LiAlSiO_4$ nano glass-ceramics for LED applications (0.5 at.% for Tb^{3+} and 0.1 at.% for Eu^{3+}) in the system Li_2O-Al_2O_3-SiO_2-$LiBO_2$ (19.6:19.6:39.1:21.7 mol%). To our knowledge this kind of investigations is not published to this moment.

EXPERIMENTAL

Li_2CO_3 (p.a.), Al_2O_3 (p.a.), SiO_2 (p.a.), H_3BO_3 (p.a.), Tb_4O_7 (p.a.) and Eu_2O_3 (p.a.) were used as raw materials. Glass syntheses were carried out in a resistive furnace with Kantal heating wire per-

mitting maximum working temperature of 1200 °C and in a chamber furnace with $MoSi_2$ heating elements allowing maximum working temperature of 1550 °C. The temperature was controlled with Pt/Pt–10%Rh thermocouple. Glasses were melted in platinum crucibles. First, the mixture was heated at 700 °C for decomposition of the lithium carbonate and boric acid and then the melt was heated at 1300 °C for three hours for homogenization. The as-obtained glass was cooled down to room temperature by quick removal from the furnace.

Different thermal analyses were done on the DTA/TG device of SETARAM Labsys evo 1600, France. The samples were investigated at a heating rate of 10 °C/min in Ar flow at a flow rate of 20 ml/min from room temperature up to 900 °C.

The prepared glasses were thermally treated for establishing of the crystallizing phases. Structural characterization was carried out by powder X-ray diffraction (XRD) using a Bruker D8 Advance powder diffractometer with Cu Kα radiation and LynxEye detector. The XRD patterns were collected at room temperature in the range from 10 to 80° 2θ. Qualitative phase analysis was performed by using Bruker EVA 2 program [36]. The mean crystallite size was calculated from the integral breadth of all peaks by using whole powder pattern fitting procedure (Pawley fit) and Scherrer equation as implemented in Bruker TOPAS 3 program [37]. The area of the amorphous phase was determined by using a straight line for a description of the background and single line for fitting the amorphous component.

The emission and excitation spectra were measured on Horiba Fluorolog 3-22 TCS spectrophotometer equipped with a 450 W Xenon Lamp as the excitation source. All spectra were measured at room temperature.

RESULTS AND DISCUSSION

Figure 1 presents the DTA curves of Tb^{3+} doped and Eu^{3+} doped precursor glasses. The glass transition temperature (Tg), crystallization onset (Tx) and crystallization temperature (Tc) appear at 510, 567 and 630 °C for the first one and 502, 555 and 623 °C for the latter one. Glass stability parameters Tx-Tg are 57 and 53 °C respectively. Therefore, glasses show not high thermal stability. We choose two different temperatures for thermal treatment – 580 and 630 °C. The first is near the crystallization onset and the second is near the exothermic peak of crystallization.

The XRD phase analyses show that the main crystallizing phase after thermal treatment with different duration and time is $LiAlSiO_4$ in two different crystallographic modifications – hexagonal
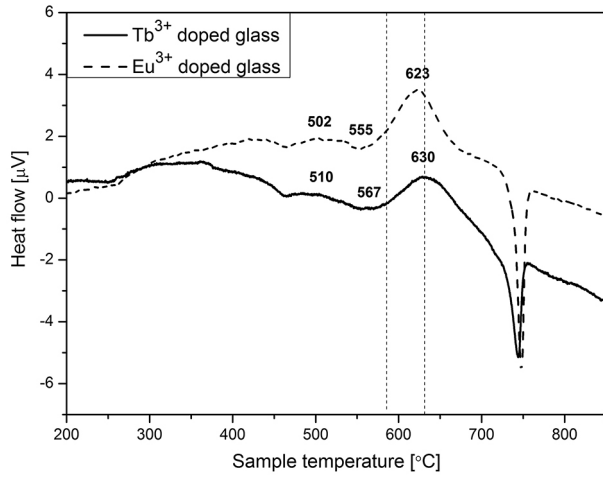
Fig. 1. DTA curves of Tb^{3+} doped and Eu^{3+} doped precursor glasses.
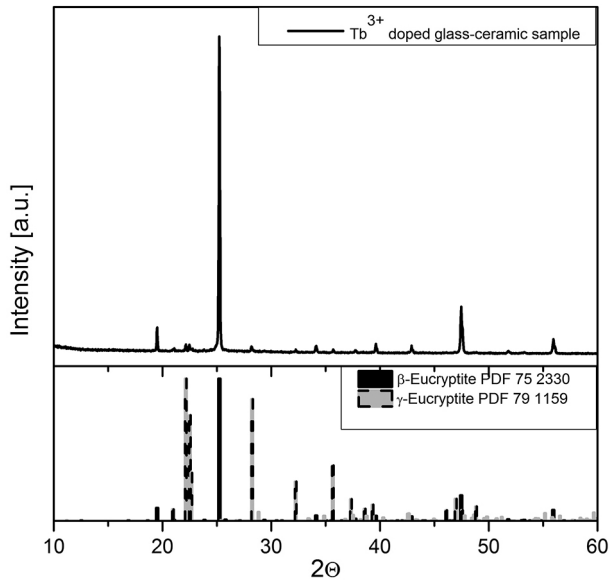
Fig. 2. XRD patterns of Tb^{3+} doped precursor glass treated at 630 °C 24 hours.

Fig. 3. XRD patterns of Tb^{3+} doped (*a*) and Eu^{3+} doped (*b*) glass-ceramic samples obtained at different thermal treatment regime. The main crystalline phase (> 95%) is Eucryptite.

The degree of crystallinity for all samples is about 90%. The crystallite size depends slightly on the rare earth ion and varies between 80 and 120 nm according to the thermal treatment regime. The crystallite sizes of the samples under consideration are presented in Table 1.

β-Eucryptite (PDF # 75-2330, SG *P6_22*) and monoclinic Pseudo-eucryptite (PDF # 79-1159, SG *Pa*), also called γ-Eucryptite. The ratio between these two phase modifications depends on the nature of the rare earth ion. After longer thermal treatment the quantity of γ -eucryptite decreases. The quantity of additional phases in the glass-ceramic samples is less than 5%. Figure 2 presents as an example the XRD patterns of Tb^{3+} doped precursor glass treated at 630 °C for 24 hours. XRD patterns of Tb^{3+} doped and Eu^{3+} doped glass-ceramic samples obtained at different thermal treatment regime are presented on Figure 3.

Table 1. Particle sizes of Tb^{3+} doped and Eu^{3+} doped glass-ceramic samples obtained at different thermal treatment regime

Sample	Particle size [nm]	Sample	Particle size [nm]
Tb 0.5 at%,580 °C		Eu 0.1 at%, 580 °C	
2 h	95	2 h	88
5 h	96	5 h	92
24 h	109	24 h	95
Tb 0.5 at%, 630 °C		Eu 0.1 at%, 630 °C	
2 h	109	2 h	97
5 h	108	5 h	98
24 h	114	24 h	107

The excitation and emission spectra of the glass-ceramic samples are presented on Figures 4 and 5.

The Tb^{3+} excitation spectrum in the range from 300 to 500 nm shows characteristic transitions of Tb^{3+}, attributed to the f–f transitions. The strongest peak is located at 379 nm corresponding to the $^{7}F_{6} \rightarrow {}^{5}D_{3}$ transition. The main emission peak of Tb^{3+} is $^{5}D_{4} \rightarrow {}^{7}F_{5}$ transition at 545 nm, correspond-
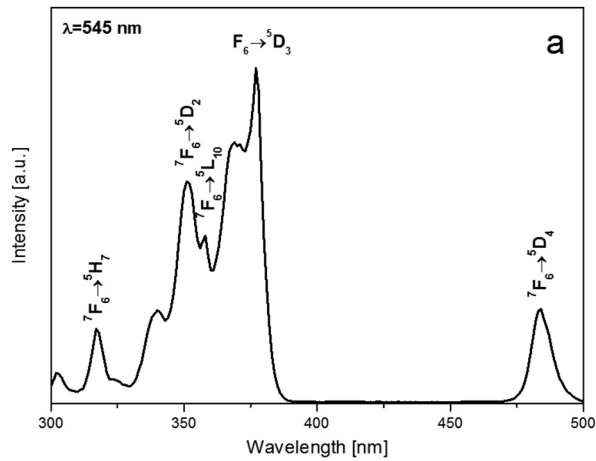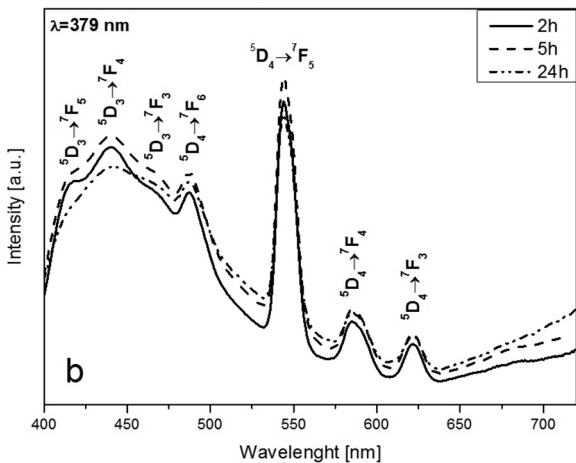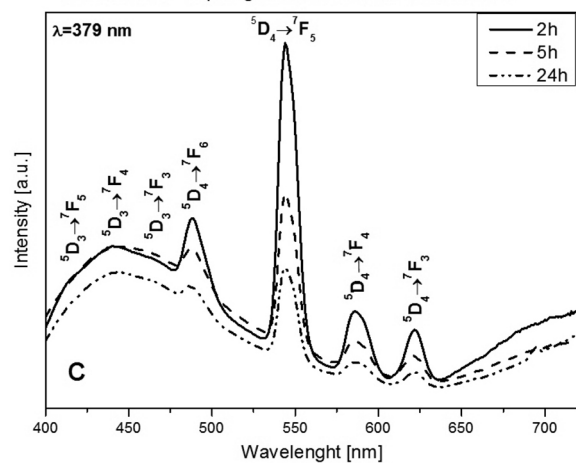
Fig. 4. (*a*) Excitation spectrum of Tb^{3+} doped glass-ceramic sample treated at 630 °C 2 h; (*b*) Emission spectra of the Tb^{3+} doped glass-ceramic samples thermal treated at 580 °C 2, 5 and 24 h; (*c*) Emission spectra of the Tb^{3+} doped glass-ceramic samples thermal treated at 630 °C 2, 5 and 24 h.
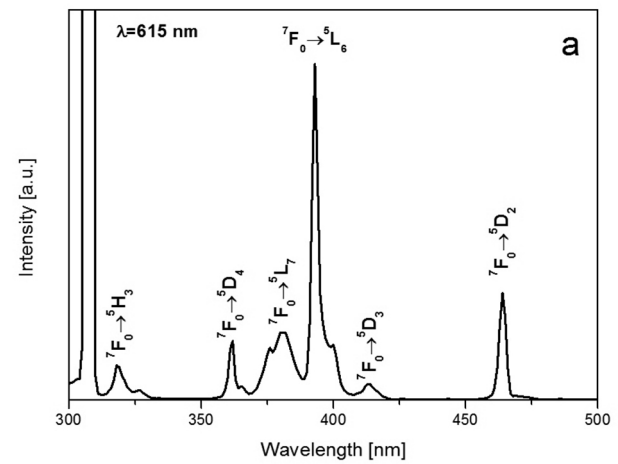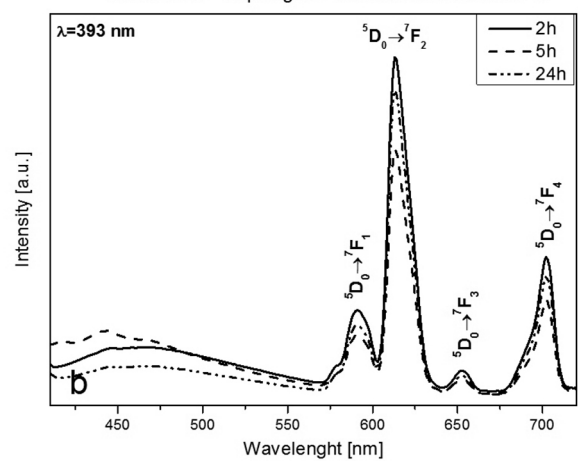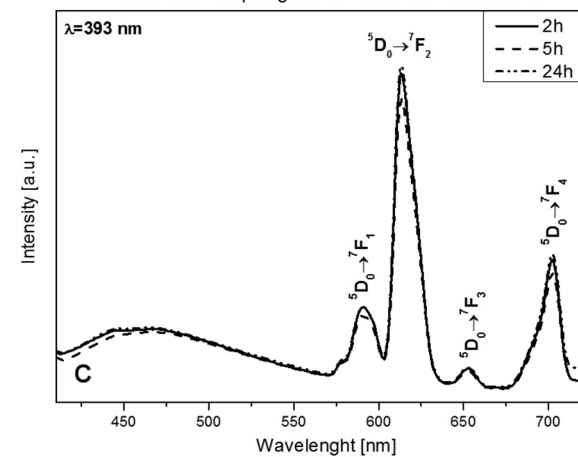
Fig. 5. (*a*) Excitation spectrum of Eu^{3+} doped glass-ceramic sample treated at 630 °C 2 h; (*b*) Emission spectra of the Eu^{3+} doped glass-ceramic samples thermal treated at 580 °C 2, 5 and 24 h; (*c*) Emission spectra of the Eu^{3+} doped glass-ceramic samples thermal treated at 630 °C 2, 5 and 24 h.

ing to the green color. Other transitions are located at 417 ($^5D_3 \rightarrow {}^7F_5$), 440 ($^5D_3 \rightarrow {}^7F_4$), 465 ($^5D_3 \rightarrow {}^7F_3$), 488 ($^5D_4 \rightarrow {}^7F_6$), 586 ($^5D_4 \rightarrow {}^7F_4$) and 621 ($^5D_4 \rightarrow {}^7F_3$) nm.

The Eu^{3+} excitation spectrum in the range from 300 to 500 nm shows characteristic transitions of Eu^{3+}, attributed also to the f–f transitions. The strongest peak is located at 393 nm corresponding to the $^7F_0 \rightarrow {}^5L_6$ transition. The main emission peak of Eu^{3+} is $^5D_0 \rightarrow {}^7F_2$ transition at 613 nm, corresponding to the orange-red color. Other transitions are located at 590 ($^5D_0 \rightarrow {}^7F_2$), 653 ($^5D_0 \rightarrow {}^7F_3$) and 702 ($^5D_0 \rightarrow {}^7F_4$) nm. As the dominant peak in the spectra is due to the $^5D_0 \rightarrow {}^7F_2$ electric dipole transition, the Eu^{3+} ion is located at the site without inversion symmetry.

Emission and excitation spectra of the glass-ceramics show the characteristic peaks of Tb^{3+} and Eu^{3+}.

Figure 6 and Table 2 present the CIE coordinates of the Tb^{3+} doped and Eu^{3+} doped glass-ceramic
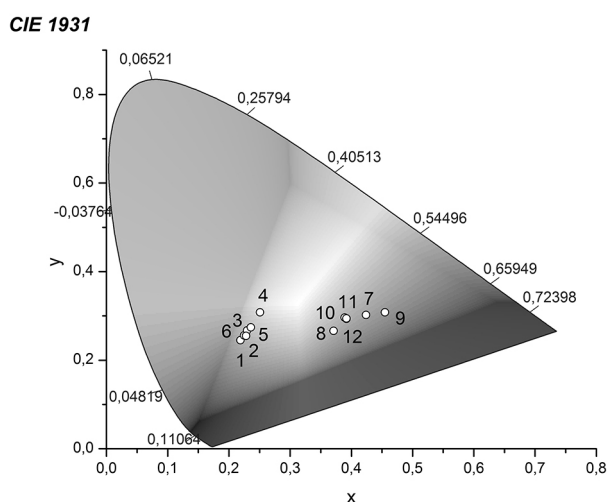
Fig. 6. CIE coordinates of the Tb^{3+} doped and Eu^{3+} doped glass-ceramic samples obtained at different thermal treatment regime.

Table 2. CIE coordinates of the Tb^{3+} doped and Eu^{3+} doped glass-ceramic samples obtained at different thermal treatment regime

Sample	Particle size [nm]	Sample	Particle size [nm]
Tb 0.5 at%, 580 °C		Eu 0.1 at%, 580 °C	
2 h	95	2 h	88
5 h	96	5 h	92
24 h	109	24 h	95
Tb 0.5 at%, 630 °C		Eu 0.1 at%, 630 °C	
2 h	109	2 h	97
5 h	108	5 h	98
24 h	114	24 h	107

samples obtained at different thermal treatment regimes. As can be seen, the CIE coordinates of the samples show different emission colors which depend on the nature of the active ion and the thermal treatment regime.

CONCLUSION

Terbium doped and europium doped glasses from the system Li_2O-Al_2O_3-SiO_2-$LiBO_2$ are prepared with a concentration of the dopants 0.5 at% for Tb^{3+} and 0.1 mol% for Eu^{3+}. Glass-ceramics are obtained after thermal treatment of the parent glass at two different temperatures and three different durations of treatment. The crystallizing phases, the degree of crystallinity and the particle size are determined. The main crystallizing phase after thermal treatment is $LiAlSiO_4$ in two different crystallographic modifications – β-Eucryptite and γ-Eucryptite. The ratio between these two phase modifications depends on the nature of the rare earth ion. After longer thermal treatment γ-Eucryptite transforms almost completely in β-Eucryptite. The quantity of additional crystalline phases is less than 5%. The degree of crystallinity for all samples is about 90%. The particle size varies between 80 and 120 nm according to the thermal treatment regime depending slightly on the Rare Earth ion nature.

Emission and excitation spectra of the glass-ceramics show the characteristic peaks of Tb^{3+} and Eu^{3+}. The main emission peak of Tb^{3+} is $^5D_4 \rightarrow {}^7F_5$ transition at 545 nm, corresponding to green color. The Tb^{3+} excitation spectrum, shows characteristic transitions of Tb^{3+}, attributed to the f–f transitions. The strongest peak is located at 379 nm corresponding to the $^7F_6 \rightarrow {}^5D_3$ transition. The main emission peak of Eu^{3+} is $^5D_0 \rightarrow {}^7F_2$ transition at 613 nm, corresponding to orange-red color. The Eu^{3+} excitation spectrum shows characteristic transitions of Eu^{3+}, attributed to the f–f transitions. The strongest peak is located at 393 nm corresponding to the $^7F_0 \rightarrow {}^5L_6$ transition. CIE coordinates of the samples show different emission colors, which depend on the active ion and thermal treatment regime. The obtained results show that as-prepared terbium doped glass-ceramics could be used as a blue-green phosphor. Europium doped glass-ceramics could be used as an orange-red phosphor. Different emission colors could be obtained by using different thermal treatment regimes.

REFERENCES

1. C. C. Lin, R.S. Liu, *J. Phys. Chem. Lett.*, **2**, 1268 (2011).
2. M. S. Shur, R. Zukauskas, *Proceedings of the IEEE*, **93**, 1691 (2005).

3. D. Wei, Y. Huang, S. Kim, Y. Yu, H. Seo, *Mater. Lett.*, **99**, 122 (2013).
4. I. Sabikoglu, M. Ayvacıklı, A. Bergeron, A. Ege, N. Can, *J. Lumin.*, **132**, 1597 (2012).
5. Y. P. Naik, M. Mohapatra, N. D. Dahale, T. K. Seshagiri, V. Natarajan, S. V. Godbole, *J. Lumin.*, **129**, 1225 (2009).
6. D. S. Jo, Y. Luo, K. Senthil, K. Toda, B. S. Kim, T. Masaki, D. H. Yoon, *Opt. Mater*., **34**, 696 (2012).
7. M. Nayak, T. R. N. Kutty, *Mater. Chem. Phys.*, **57**, 138 (1998).
8. G. U. O. Yuzhu, Y. U. Xibin, L. I. U. Jie, Y. Xuyong, *J. Rare Earth*, **28**, 34 (2010).
9. J. Dhoble, B. P. Kore, A. N. Yerpude, R. L. Kohale, P. W. Yawalkar, N. S. Dhoble, *Optik*, **126**, 1527 (2015).
10. A. Kumar, S. J. Dhoble, D. R. Peshwe, J. Bhatt, *J. Alloys Compd.*, **609**, 100 (2014).
11. Q. Lu, J. Li, D. Wang, *Curr. Appl. Phys.*, **13**, 1506 (2013)
12. K. Li, S. Liang, H. Lian, M. Shang, B. Xing, J. Lin, *J. Mat. Chem. C*, **4**, 3443 (2016).
13. L. Wenzhen, G. Ning, J. Yongchao, Z. Qi, Y. Hongpeng, *Opt. Mater.*, **35**, 1013 (2013).
14. Y. Liu, X. Zhang, Z. Hao, Y. Luo, X. Wang, L. Ma, J. Zhang, *J. Lumin.*, **133**, 21 (2013).
15. J. Zhou, T. Wang, X. Yu, D. Zhou, J.i Qiu, *Mat. Res. Bull.*, **73**, 1 (2016).
16. S. Shionoya, W. M. Yen, H. Yamamoto (eds.), Phosphor handbook, CRC press, 2006.
17. P. Babu, K. H. Jang, C. S. Rao, L. Shi, C. K. Jayasankar, V. Lavín, H. J. Seo, *Opt. Express*, **19**, 1836 (2011).
18. R. Krsmanović, S. Bals, G. Bertoni, G. Van Tendeloo, *Opt. Mater.*, **30**, 1183 (2008).
19. D. Chen, W. Xiang, X. Liang, J. Zhong, H. Yu, M. Ding, Z. Ji, *J. Eur. Ceram. Soc.*, **35**, 859 (2015).
20. R. Krsmanović, S. Bals, G. Bertoni, G. V. Tendeloo, *Opt. Mater*., **30**, 1183 (2008).
21. M. A. N. Xiaoqin, Y. U. Lixin, S. U. N. Jiaju, L. I. Songchu, J. Zhong, *J. Rare Earths*, **35**, 446 (2017).
22. E. Trusova, A. Vaitkevičius, Y. Tratsiak, M. Korjik, P. Mengucci, D. Rinaldi, L. Montalito, V. Marciulionyte, G. Tamulaitis, *Opt. Mater.*, **84**, 459 (2018).
23. H. Bouchouicha, G. Panczer, D. de Ligny, Y. Guyot, R. Ternane, *Opt. Mater.*, **85**, 41 (2018).
24. N. Dai, H. Luan, Z. Liu, Y. Sheng, J. Peng, Z. Jiang, J. Li, *J. Non-Cryst. Solids*, **358**, 2970 (2012).
25. R. S. Liu (ed.), Phosphors, Up Conversion Nano Particles, Quantum Dots and Their Applications, Vol. 1, Springer, 2016. ISBN: 978-3-662-52769-6 (Print) 978-3-662-52771-9 (Online).
26. I. Koseva, P. Tzvetkov, A. Yordanova, M. Marychev, O. Dimitrov, V. Nikolov, *Bulg. Chem. Commun*., **49**, 366 (2017).
27. V. Correcher, L. Sanchez-Munoz, J. Garcia-Guinea, J. M. Gomez-Ros, A. Delgado, *Nuc. Instrum. Meth. A*, **562**, 456 (2006).
28. H. G. F. Winkler, *Acta Cryst.*, **1**, 27 (1948).
29. R. Roy, D. M. Roy, E. F. Osborn, *J. Am. Ceram. Soc.*, **33**, 152 (1950).
30. H. Schulz, V. Tscherry, *Acta Cryst. B*, **28**, 2174 (1972).
31. W. I. Abdel-Fatah, M. S. Fayed, S. R. Gooda, W. F. F. Mekky, *J. Sol–Gel Sci. Techn.*, **13**, 981 (1998).
32. J. H. Westbrook, *J. Am. Ceram. Soc.*, **41**, 433 (1958).
33. P. Norby, *Zeolites*, **10**, 193 (1990).
34. B. E. Douglas, S. M. Ho, in: Structure and Chemistry of Crystalline Solids, Springer, ISBN-10: 0-387-26147-8; ISBN-13: 978-0387-26147-8, 2006, p. 253
35. U. B. Gokhe, K. A. Koparkar, S. K. Omanwar, *J. Alloys Compd.*, **689**, 992 (2016).
36. Bruker AXS (2009) EVA 2, DIFFRACplus Evaluation Package.
37. Bruker AXS (2005) TOPAS V3, General profile and structure analysis software for powder diffraction data.